

SUPPORTING INFORMATION

Self-Assembled, Nacre-Mimetic, Nano-lamellar Structure as a Superior Charge Dissipation Coating on Insulators in HVDC Gas-Insulated System

Boya Zhang,^{*,a} Qiang Wang,^{*,b} Yunxiao Zhang,^c Wenqiang Gao,^c Yicen Hou,^c and

Guixin Zhang^c

^aState Key Laboratory of Electrical Insulation and Power Equipment, School of Electrical Engineering, Xi'an Jiaotong University, Xi'an 710049, China

^bSchool of Mechatronic Engineering, Beijing Institute of Technology, Beijing 100081, China

^cDepartment of Electrical Engineering, Tsinghua University, Beijing 100084, China

*corresponding author: zhangby@xjtu.edu.cn; wang_qiang@bit.edu.cn

1. Materials

Poly(vinyl alcohol) (PVA) (Mw: 27000, 87-89% hydrolysis, Macklin Biochemical, China), glutaraldehyde (GA) (50 wt% solution, Mw: 100.12, Sangon Biotech, China), and hydrochloric acid (HCl) (36~38 wt% solution, Tong-Guang Fine Chemicals, China) were purchased in the highest purity and used as received. Sodium coordinated montmorillonite (MMT) clay with a specific surface area of ~240 m²/g was purchased from Yuanye Biotech, China. High-purity deionized water was used in all experiments.

The substrates for this study were 400- μ m-thick epoxy insulating plates and cone-type insulators. The insulating plates were used as samples, cast from glycidyl ether type epoxy resin ER113 (DOW Chemical, USA) and anhydride curing agent EH314 (DOW Chemical, USA) according to a procedure reported elsewhere.¹ The cone-type insulators were made of α -Al₂O₃-filled epoxy resin, manufactured by Taikai Group Co., Ltd., using the same material formulation and manufacturing process for cone-type insulators in high voltage GIL and GIS.

2. Sample Preparation

Adsorption of a single polymer layer onto clay platelets. First, a 1 wt% dispersion of MMT clay in deionized water was prepared by intense stirring for one week. This solution was allowed to precipitate for 24 hours. After discarding the sediment, the supernatant fraction was ultra-sonicated for 15 min (OuHor UH550-T, 550W, 20 kHz) to fully exfoliate MMT clay into individual monolayer nanosheets. Meanwhile, PVA was dissolved in de-ionized water with the assistance of brief heating. To adsorb one monolayer polymer onto the clay platelets, the PVA solution was slowly added to the MMT dispersion until a weight ratio of 50/50 (w/w) PVA/MMT and a concentration of 1.5 wt% was achieved. To insure a uniform dispersion, the mixture was carefully stirred for 30 min and ultra-sonicated for 10 min. Next, a small amount of crosslinking agent GA and catalyst HCl (mole ratio of HCl:GA=1:5) was added to the mixture in order to covalently incorporate the MMT nanosheets into the PVA matrix. Finally, the solution was stirred for at least overnight to complete the polymer adsorption and ensure a fine dispersion of the stabilized MMT nanosheets.

Dip coating. In order to enhance the adhesion of substrate and the PVA/MMT dispersion, all the substrates were pre-treated by a primer PVA layer to increase the hydrophilicity. Then, the samples were coated by simply dipping them into the above aqueous dispersion for about 60 seconds, and then hung vertically in a vacuum oven to be degassed, dried and crosslinked overnight at 60 °C. The coating process can be repeated several times to obtain a coating layer of desired thickness.

3. Materials Characterization

3.1 Instrument Specifications

Fourier Transform Infrared (FTIR) spectra were recorded in the attenuated total reflectance (ATR) mode using a ZnSe crystal as a contact to the samples with a Nicolet Magna-IR 560 spectrometer.

X-ray Photoelectron Spectroscopy (XPS) was performed using a PHI Quantera SXM scanning X-ray microprobe system with a base pressure of 1×10^{-7} torr. Al K α excitation radiation was used as the X-ray source with a pass energy of 55 eV, 45° takeoff angle and a 200 μm beam size. All of the survey spectra were recorded in 0.1 eV step size and calibrated using the binding energy (284.6 eV) of C1s peak.

Transmission Electron Microscopy (TEM) was performed on a JEOL JEM-F200 TEM at an acceleration voltage of 200 kV. Microtomed ultrathin sections of the coated epoxy sample were obtained using a Leica EM UC7/FC7 Cryo-Ultramicrotome. High-angle annular dark field-scanning transmission electron microscopy (HAADF-STEM) image and the corresponding energy dispersive X-ray (EDX) mapping were also obtained from the JEOL JEM-F200. The ImageJ software was used for digital imaging processing and analysis.

X-ray Diffraction (XRD) patterns were collected using a Bruker D5005 diffractometer with Bragg Brentano geometry using Cu K α radiation ($\lambda=1.5418\text{\AA}$) at 40 kV voltage and 40 mA current. The samples were measured in the angular range (2θ) 1.5° to 30° at a scanning step of 0.1°.

3.2 Supplementary characterization results

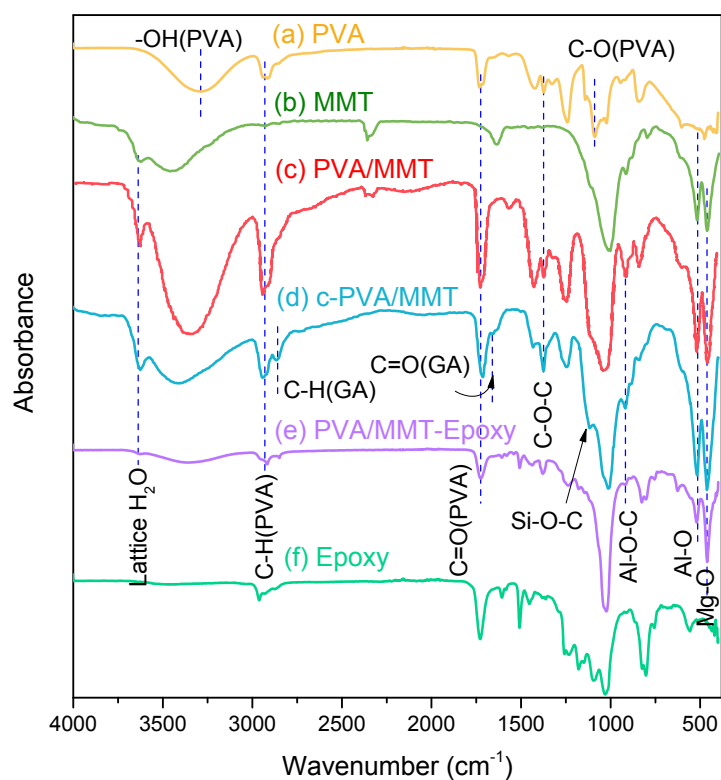


Fig. S1 FTIR spectra analysis. (a) pure PVA, (b) pure MMT, (c) non-cross-linked PVA/MMT composites, (d) cross-linked PVA/MMT composites, (e) PVA/MMT coating on an epoxy substrate, (f) pure epoxy. The presence of the typical bands of PVA (3270-3400 cm^{-1} , -OH stretching; 2940 cm^{-1} , C-H stretching; 1735 cm^{-1} , C=O stretching from the acetate groups; 1095 cm^{-1} , C-O stretching) and MMT (3630 cm^{-1} , -OH stretching of lattice water; 1050-1000 cm^{-1} , Si-O stretching; 518 cm^{-1} Al-O stretching; 468 cm^{-1} Mg-O stretching) are confirmed.

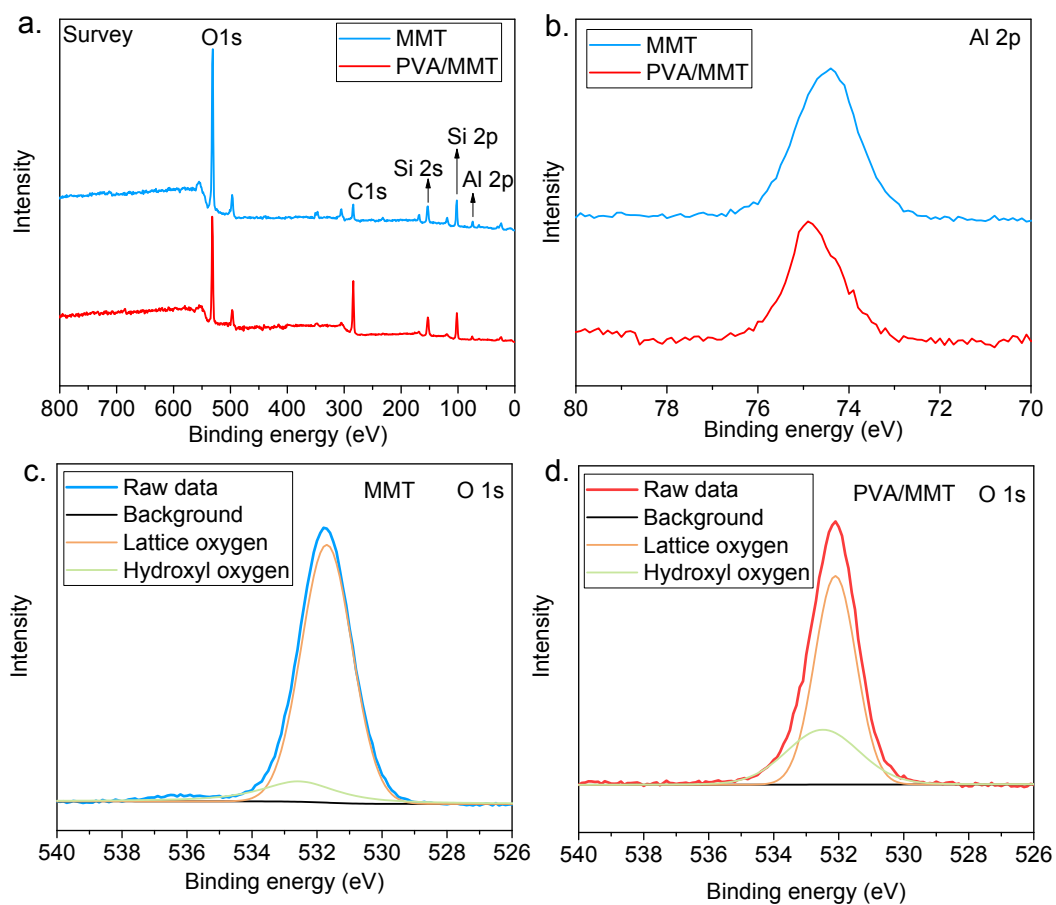


Fig. S2. XPS spectra analysis. (a) survey spectrum and (b) high-resolution Al 2p spectrum in pure MMT and PVA/MMT coating; (c) O 1s spectrum in pure MMT; (d) O 1s spectrum in PVA/MMT coating.

4. Electrical Property Characterization

4.1 Surface potential measurement

A “needle-to-plane” electrode is used for charging the insulator, as shown in Fig. S3a. A positive dc corona ($U= +5$ kV) occurs at the tip of the needle with a separation of 8 mm above the sample center. The sample is first corona charged for one minute and then transferred to the surface potential measurement platform, as shown in Fig. S3b. A Kelvin probe (Trek 3455ET) is fixed on a XY linear stage and connected to an electrostatic voltmeter (Trek 341B). The stage is controlled by a programmable motion controller, and the output signal from the probe is collected by a 12-bit oscilloscope (LeCory HDO4034). In the test, an area of 32 mm×32 mm is scanned in a raster mode, with a step of 0.5 mm between each collecting point.

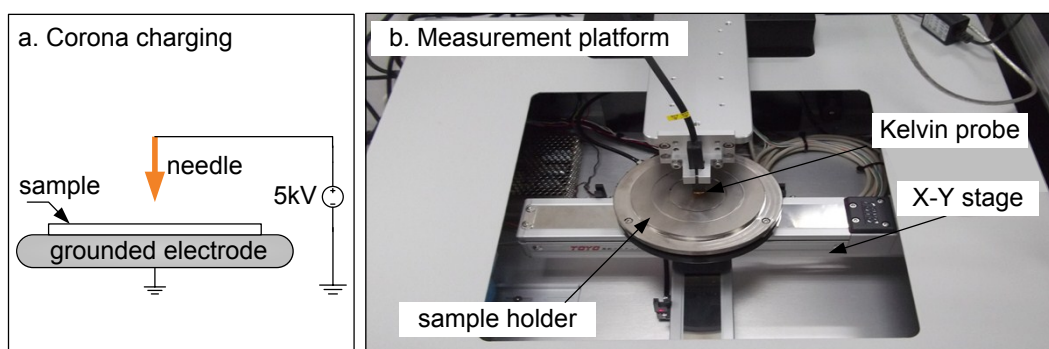


Fig. S3 Surface potential measurement on insulators after corona charging.

4.2 Trap level distribution measurement

Isothermal surface potential decay (ISPD) test is adopted to characterize the trap level distributions of the insulators. The sample is first charged by a corona source using a “needle-grid to surface” structure (Fig. S4a). The needle and the mesh grid are applied with ± 12.5 kV and ± 3 kV dc voltage, respectively. The mesh grid is interposed 30 mm below the needle and 5 mm above the sample surface, so that the sample can be charged uniformly to the grid potential. After charged for 3 min, the sample is moved to the Kelvin probe (Trek 3455ET) in 2 seconds via a rotatable platform and the surface potential decay curve under room temperature can be recorded. Fig. S4b shows the normalized isothermal potential decay curves $\phi(t)$ of coated sample and uncoated sample after positively and negatively charged.

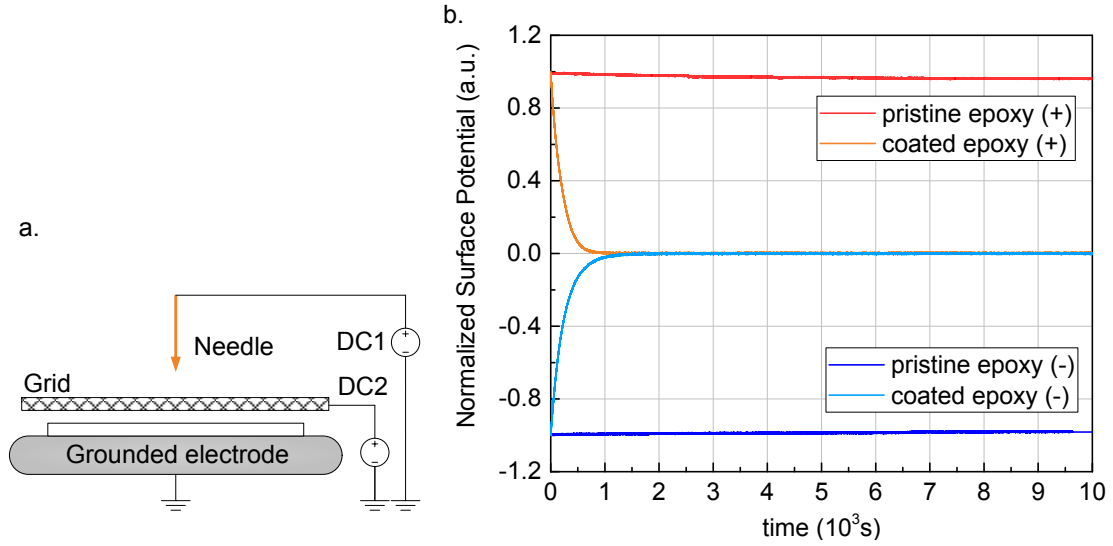


Fig. S4 (a) The “needle-grid to surface” electrode configuration for charging the sample surface. (b) Normalized isothermal potential decay curves of pristine and coated epoxy insulators after positive (+) and negative (-) corona charging.

Based on the theory of isothermal discharge current (IDC) proposed by Simmons, the density of traps $N(E_T)$ and the energy of traps E_T can be calculated by following equations.²

$$N(E_T) = \frac{\varepsilon t}{q_e f_0 k T \delta L} \frac{d\varphi(t)}{dt} \quad (1)$$

$$E_T = kT \ln(\gamma t) \quad (2)$$

where ε is the permittivity of the sample and L is the thickness of the sample. δ is the penetration depth of injected electrons. q_e is the elementary charge quantity. k is the Boltzmann constant. T is the absolute temperature (303 K). γ is the escape frequency of trapped electrons, which is approximately equal to 10^{12} s^{-1} . f_0 is the rate of initial occupancy of traps. Here, we assume $f_0=1$ for simplification.

During the isothermal potential decay process, charges in lower trap detrapp first and then those in deeper trap detrapp later. In other words, the release time of charges corresponds to its trap depth. Therefore, considering shallow traps and deep traps, it can be assumed that there are two types of decay process occurring simultaneously.³ Therefore, a double exponential decay equation is applied in this study to fit the decay curves: $\varphi(t) = a_1 e^{-b_1 t} + a_2 e^{-b_2 t}$, where a_1, b_1, a_2, b_2 are the fitting parameters.

4.3 DC conductivity measurement

High field conductive characteristics of samples with a thickness of 400 μm are measured at room temperature, following a standard procedure using a three-electrode system under a dc field of 15 kV/mm. The diameters of the high voltage electrode and main electrode are 25 and 20 mm, respectively. The inner diameter of the cylindrical guard electrode is 22 mm. Currents are recorded by a high resolution electrometer (Keithley 6517B) for 600 s. Then the volume conductivity (κ_v) and surface conductivity (κ_s) can be obtained by the following two equations, respectively.

$$\kappa_v = \frac{I}{U} \frac{4h}{\pi(d+g)^2}, \quad \kappa_s = \frac{I}{U} \frac{g}{\pi(d+g)} \quad (3)$$

where I is the mean value of the charging current during the final 60 s. U is the applied voltage. d is the diameter of the main electrode and g is the gap distance between the main electrode and guard electrode. h is the thickness of the sample. It should be note that for each value of conductivity, three samples are used to get the average value.

4.4 Surface charge measurement based on a downscaled GIL unit

The tested insulators are cone-type model insulators, made of alumina-epoxy composites. The thickness of the insulator is 17.5 mm; the outer and inner diameter is 100 mm and 12 mm, respectively. The insulator, the grounded enclosure and the high voltage conductor together forms a downscaled GIL unit (Fig. S5a). The resulting electric field distribution of the unit under 20 kV is shown in Fig. S5b.

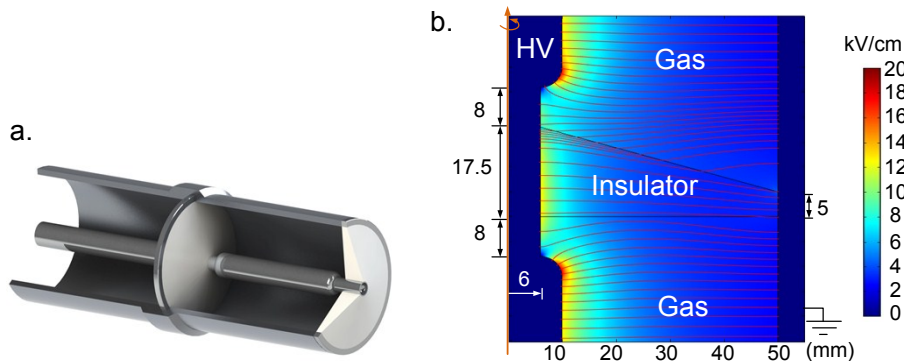


Fig. S5 (a) The electrode configuration of the downscaled GIL unit; (b) the resulting electric field distribution.

Fig. S6a shows the schematic diagram of the surface charge measurement platform, which combines the flexible exchange of electrodes and insulators with an

accurate automated surface potential scanning system. Measurements are conducted at room temperature with relative humidity less than 5%. Before each measurement, the model insulator is dried at 70 °C for at least 24 h. After installation, the cone-type insulator is cleaned with isopropanol to remove the original surface charge.

A Kelvin probe (Trek 555-P) and an electrostatic voltmeter (Trek 347) are used to measure the surface potential of the insulator. The measurement process is completed automatically by a 4-axis motion control platform in a sealed chamber (Fig. S6b). After the high voltage is switched-off, the GIL unit is opened by the linear translation stage X1 and X2. Then, as the probe moves along the radius of the insulator with the help of T1, the insulator is rotated cooperatively by the rotation stage Θ , so that the entire surface of insulator can be scanned with a spiral trajectory. The measured data is recorded by an oscilloscope (LeCory HDO4034). The sampling step in the rotation and radial direction was 1° and 1 mm, respectively, so that the insulator surface was divided into $N=360 \times 44$ elements.

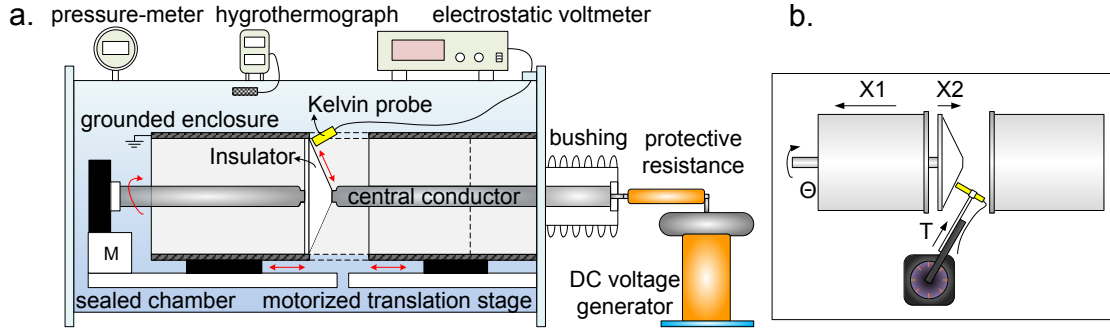


Fig. S6 (a) Schematic diagram of the surface charge measurement platform; (b) illustration of the measurement processes.

It should be noted that the surface potential measurement on one element is determined by all the charges on the tested surface. The measured potential ϕ , therefore, corresponds to the linear superimposition of the effect of all the surface charges σ , which can be expressed as:

$$\phi_{N \times 1} = \mathbf{H}_{N \times N} \sigma_{N \times 1} = \begin{pmatrix} h_{11} & L & h_{1N} \\ M & O & M \\ h_{N1} & L & h_{NN} \end{pmatrix} \begin{pmatrix} \sigma_1 \\ M \\ \sigma_N \end{pmatrix} \quad (4)$$

where the element h_{ij} in \mathbf{H} is the measured potential on point i attributed to a unit charge on the point j . The N^2 components in matrix \mathbf{H} can be obtained by electrostatic

field simulation for 44 runs, taking into account the circular symmetry of the insulator.

To get the surface charge density distribution, inversion calculation of equation (4) should be performed. To eliminate the ill-conditioned problem during the inversion calculation, Tikhonov regularization method is applied to calculate the distribution of surface charge density $\hat{\sigma}$, as shown in equation (5).⁴

$$\hat{\sigma} = (\mathbf{H}^T \mathbf{H} + \alpha \mathbf{I})^{-1} \mathbf{H}^T \boldsymbol{\varphi} \quad (5)$$

where, \mathbf{I} is a unit matrix, and α is the regularization parameter.

4.5 Flashover test

The classical finger-shaped electrode configuration is used to measure the flashover voltage across the insulator between two electrodes. The samples (3 mm-thick) are pressed by two semicircular alumina electrodes that are fixed in a PTFE holder, as shown in Fig. S7. The radius of the electrodes is 15 mm and the distance between the two electrodes is 20 mm. The thickness of the electrodes is 5 mm. The samples are stressed by a positive dc voltage with a ramping rate of 500 V/s until flashover happens. The tests are performed in a sealed chamber with 0.1 MPa dry air.

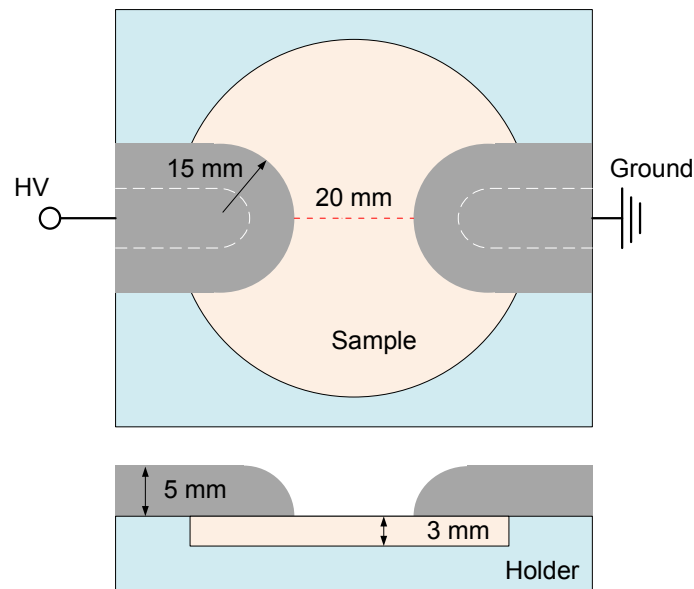


Fig. S7 Schematic diagram of the electrode configuration.

Works cited in supporting information

1. Zhang, B.Y.; Gao, W.Q.; Chu, P.F.; Zhang, Z.; Zhang, G.X. Trap-modulated carrier transport tailors the dielectric properties of alumina/epoxy nanocomposites. *J. Mater. Sci.: Mater. Electron.*, **29**(3), 1964-1974 (2018).

2. Simmons, J. G.; Tam, M. C. Theory of isothermal currents and the direct determination of trap parameters in semiconductors and insulators containing arbitrary trap distributions. *Phys. Rev. B* **7**(8), 3706-3713 (1973).
3. Zhou, T.C.; Chen, G.; Liao, R.J.; Xu, Z.Q. Charge trapping and detrapping in polymeric materials: Trapping parameters. *J. Appl. Phys.* **110**(4), 043724 (2011).
4. Zhang, B.Y.; Gao, W.Q.; Qi, Z.; Wang, Q.; Zhang G.X. Inversion algorithm to calculate charge density on solid dielectric surface based on surface potential measurement. *IEEE Trans. Instrum. Meas.*, **66**(12), 3316-3326 (2017).